Generation of broadly tunable picosecond mid-infrared laser and sensitive detection of a mid-infrared signal by parametric frequency up-conversion in MgO:$LiNbO_3$ optical parametric amplifiers*

Zhang Qiu-Lin(张秋琳)[a], Zhang Jing(张 静)[a], Qiu Kang-Sheng(邱康生)[a], Zhang Dong-Xiang(张东香)[a], Feng Bao-Hua(冯宝华)[a]†, and Zhang Jing-Yuan(张景园)[b]

[a] *Beijing National Laboratory for Condensed Matter Physics, Institute of Physics, Chinese Academy of Sciences, Beijing* 100190, *China*

[b] *Department of Physics, Georgia Southern University, Statesboro, GA* 30460, *USA*

(Received 14 December 2011; revised manuscript received 11 January 2012)

Picosecond optical parametric generation and amplification in the near-infrared region within 1.361–1.656 μm and the mid-infrared region within 2.976–4.875 μm is constructed on the basis of bulk MgO:$LiNbO_3$ crystals pumped at 1.064 μm. The maximum pulse energy reaches 1.3 mJ at 1.464 μm and 0.47 mJ at 3.894 μm, corresponding to a pump-to-idler photon conversion efficiency of 25%. By seeding the hard-to-measure mid-infrared radiation as the idler in the optical parametric amplification and measuring the amplified and frequency up-converted signal in the near-infrared or even visible region, one can measure very week mid-infrared radiation with ordinary detectors, which are insensitive to mid-infrared radiation, with a very high gain. A maximum gain factor of about 7×10^7 is achieved at the mid-infrared wavelength of 3.374 μm and the corresponding energy detection limit is as low as about 390 aJ per pulse.

Keywords: optical parametric amplifiers, picoseconds mid-infrared laser, sensitive detection

PACS: 42.65.–K, 42.65.Yj **DOI:** 10.1088/1674-1056/21/5/054213

1. Introduction

Tunable mid-infrared (MIR) coherent sources have attracted much attention due to their application in quantum optics,[1] material spectroscopy,[2,3] speckle-free imaging,[4] and air pollution detection.[5] Optical parametric generation and amplification (OPG/OPA) is an efficient approach to generating a laser with a suitable pump source and MIR nonlinear optical crystals. The nonlinear optical crystal used most often in the MIR region is MgO-doped lithium niobate ($LiNbO_3$), which combines a high optical damage threshold, large nonlinear-optical coefficients, and good transparency from the visible to the MIR region longer than 4 μm. In recent years, interest has been aroused in using periodically poled lithium niobate (PPLN) as the nonlinear crystals, whose tuning is accomplished by a change of the crystal periodicity or by a change of the crystal temperature.[6–8] Here, a simply and widely tunable MIR laser source based on OPG/OPA with bulk MgO:$LiNbO_3$ crystals is reported, which has particular advantages of being angularly tunable and operated at room temperature. The signal wavelength from 1.361 μm to 1.656 μm and idler wavelength from 2.976 μm to 4.875 μm are obtained when it is pumped at 1.064 μm, which have a much wider tuning range than previous reports of OPG/OPA with bulk MgO:$LiNbO_3$ crystals.[9–12] The tuning range can be further extended to 600.7–652.1 nm for the signal blanch and 4.65–2.889 μm for the idler blanch when the OPG/OPA is pumped at 532 nm.

The detection of weak optical signals, especially spectral components in the MIR region, is always a problem because the optical detectors are poor with low signal-to-noise ratio in the MIR region. Many detectors, such as CCD, have very low quantum yields at wavelengths longer than 1.1 μm. Fortunately, the OPA technique with a high optical gain can be adopted to amplify weak signals as a preamplifier. More importantly, the OPA not only directly amplifies the weak signal but also converts the MIR optical pulses into the near-infrared or visible range through

*Project supported by the National Natural Science Foundation of China (Grant No. 61078005), the National Basic Research Program of China (Grant No. 2007CB613205), and the China Postdoctoral Science Foundation.

†Corresponding author. E-mail: bhfeng@aphy.iphy.ac.cn

© 2012 Chinese Physical Society and IOP Publishing Ltd

idler-to-signal parametric up-conversion. In addition, it allows the indirect detection of MIR components with a very high sensitivity. Since the signal and the idler are generated and amplified in a pair and can be reconstructed both temporally and spectrally from each other, the characteristic of MIR signals can be detected in the near-infrared or visible range with high sensitivity. Carlos *et al.* have detected an MIR signal by using this technique.[13] The OPA technique used for detecting weak signals first demonstrated by Zhang and co-workers has been applied in the detection of near-infrared weak signal.[14] In this paper, we will extend this technique to the detection of a picosecond MIR weak signal. The detection limit can be as low as about 390 aJ per pulse at 3.374 μm with a gain as high as about 7×10^7.

2. Experimental arrangements

The schematic diagram of the experimental arrangement is shown in Fig. 1. A passive-active mode-locked Nd:YAG laser with a repetition rate of 10 Hz (EKSPLA, PL2143B) delivering pulses at 1.064 μm with a beam diameter of 10 mm (vertically polarized, 25 ps) is used as the pump source of the OPG/OPA. After an optical isolator (OI), the beam diameter is reduced to 3 mm by using a telescope. Then the pump beam is split into two parts by a beam splitter (BS) with a ratio of 1:1. One is used to pump an OPG/OPA stage and the other to pump an OPA after a suitable delay. At the OPG/OPA stage, a double-pass configuration is adopted, which can provide high gain and reduce the threshold. The signal beam is reflected by a silver mirror M4. By tilting the two crystals in opposite directions from the OPG axis, the beam walk-off of the pump and signal waves in the two crystals can be partially cancelled. All the $MgO:LiNbO_3$ crystals for OPG and OPA are cut at $\theta = 49°$ for type I phase matching and have a dimension of 10 mm(W) × 15 mm(H) × 40 mm(L), which can be angularly tuned synchronously in the vertical plane to achieve phase matching with the pump beam at 1064 nm linearly polarized in the vertical direction. Both end facets of the crystals are polished at an angle of 2° relative to each other to avoid back-reflection of the pump laser into the cavity and antireflection-coated for 1.064 μm, 1.3–1.7 μm, and 3–5 μm. After the OPG stage, the generated signal, separated from the residual pump beam by the CaF_2 dichroic mirror M6, serves as a seed for the OPA and then injects into the OPA to be further amplified. The pump and seed beams are combined collinearly in the $MgO:LiNbO_3$ crystal by a dichroic mirror M7, which is also highly reflective at 1.064 μm and transmission at 1.3–1.7 μm and 3–5 μm. The temporal overlap between the seed and the pump pulse is adjusted by precisely controlling an optical delay line. After the OPA stage, the pump and amplified signal beams are separated by another dichroic mirror M8. In order to up-convert the MIR signal into a visible range, a frequency-doubled Nd:YAG laser at 532 nm is used as the OPA pump source after a suitable delay. The $MgO:LiNbO_3$ crystal of C8 is cut at $\theta = 51.3°$ for type I phase matching and has a dimension of 10 mm(W) × 20 mm(H) × 25 mm(L), which can be angularly tuned synchronously in the vertical plane to achieve phase matching. After the OPA stage, the pump and amplified signal beams are separated by a CaF_2 mirror M13, which is highly reflective at 532 nm at 45°. In order to eliminate the effect of the fluctuation of the pump source, each set of data is taken from the averaged value over 50 laser shots.

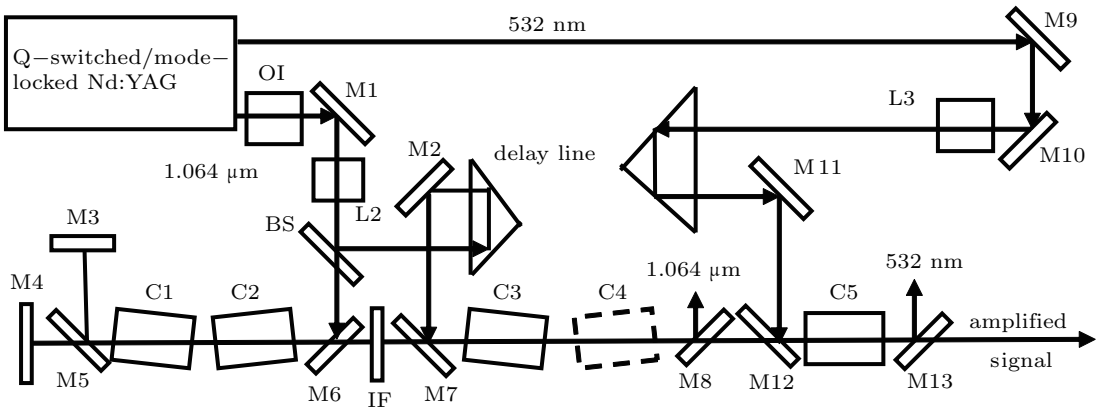


Fig. 1. Schematic diagram of the experimental setup. OI: optical isolator; L2-L3: lens system; C1–C4: $MgO:LiNbO_3$ crystals for 1064 nm pumped OPA; C5: 532 nm pumped $MgO:LiNbO_3$ OPA crystal; BS: beam splitter; M1, M2: mirrors, HR@1.064 μm at 45°; M3: mirrors, HR@1.064 μm at 0°; M4: silver mirror; M5–M8: CaF_2dichroic mirrors, HR@1.064 μm and HT@1.3–1.7 μm, 3–5 μm at 45°; IF: 3.2 μm IR long pass filter; M9–M11: mirrors, HR@532 nm at 45°; M12, M13: CaF_2 mirrors, HR@532 nm at 45°.

3. Results and discussion

3.1. Characteristics of the OPG/OPA output

A widely tunable MIR radiation source is obtained after optimization of the temporal/spatial overlap and the phase-matching condition. The output energy of the OPG/OPA as a function of wavelength is shown in Fig. 2. The generated idler energy is deduced from the Manley–Rowe equation. The output signal can be continuously tuned from 1.361 to 1.656 μm, whereas the idler changed from 4.875 to 2.976 μm. Under total pump energy of 6.8 mJ, which corresponds to a pump intensity of 1.9 GW/cm^2, the maximum signal output energy is approximately 1.3 mJ per pulse at 1.464 μm, whereas the corresponding idler energy at 3.894 μm is approximately 0.47 mJ per pulse. In addition, the quantum conversion efficiency from the pump to the generated MIR signal is higher than 25%, which is considerably large since picoseconds OPG/OPA generation starts from the quantum noise.

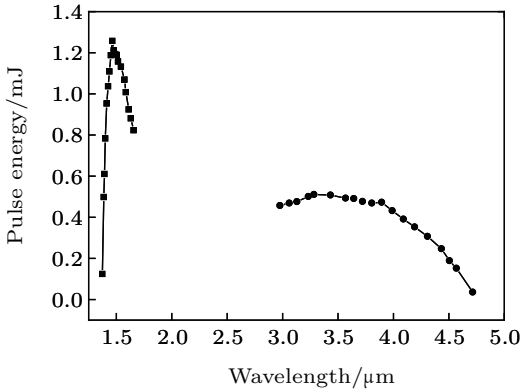


Fig. 2. Output pulse energy of the 1064 nm pumped OPG/OPA as a function of wavelength. The squares are the outputs of the signal branch and the dots are the idler branch.

The spectral property of the signal radiation is shown in Fig. 3, which is measured with a fiber spectrometer with a spectral range of 0.85–2.5 μm. The spectrometer is unable to cover the spectral range of the MIR region beyond 2.5 μm. However, the spectral characters of that part of the MIR region can be deduced from Fig. 3, and it is quite reasonable since the signal and idler photons are created in pairs. In addition, the relative intensity of the signal line is in accordance with the signal pulse energy, which has a maximum value at 1.464 μm (idler wavelength at 3.894 μm). The intensity drops with the decline of the pump pulse energy till the signal lines cannot be detected with the fiber spectrometer, which is defined as the threshold. In this method, the threshold pump intensity for 1.464 μm (idler wavelength at 3.894 μm) is found to be as low as 670 MW/cm^2 , corresponding to the pump pulse energy of 2.4 mJ. The intensity of the signals at the tuning edges declines and the signal wavelength cannot be tuned beyond 1.361 μm, corresponding to an idler wavelength at 4.875 μm due to the optical absorption at the idler wave by the MgO:LiNbO$_3$. The data in Fig. 3 show that the radiation in the MIR components can be up-converted to the near-IR range for detection using a detector in the near-IR region.

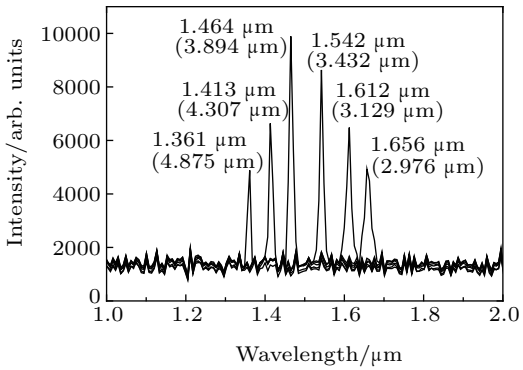


Fig. 3. Typical spectra of the up-converted signal radiation of the 1064 nm pumped OPA when it is seeded with an idler radiation in the mid-IR region, showing the effectiveness of parametric up-conversion. The corresponding seeding wavelength of each peak is marked in the brackets.

The up-converted radiation in the near-IR region is sometimes difficult to detect effectively in some detectors, such as CCD, which is insensitive to radiation longer than 1.1 μm. Therefore, up-conversion to the visible range is very useful for those detectors. The MIR signal can also be up-converted to the visible range by seeding the MIR pulse in a MgO:LiNbO$_3$ OPA pumped at 532 nm. The spectral property of the visible range is detected by a fiber spectrometer (spectrum region: 200–1100 nm), which is shown in Fig. 4. By using this OPA stage, the wavelength range covers from 600.7 nm to 652.1 nm, corresponding to the MIR seeds from 2.888 μm to 4.651 μm.

Figure 5 shows the dependence of the pulse energy at a wavelength of 3.374 μm on the relative time delay between the pump of the OPA and the seeds generated from OPG after being spatially filtered by using a pinhole with diameter of 1 mm, a series optical density filters (ODF) and a 3.2 μm IR long pass filter. As shown in the figure, the curve exhibits a pulse duration of about 16 ps, which is shorter than the pump source.

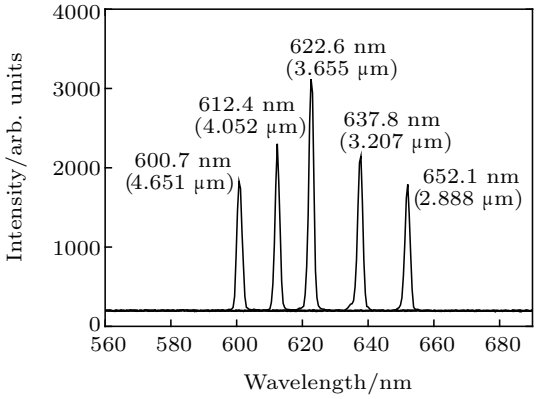


Fig. 4. The visible spectra for the up-converted MIR radiation in a 532 nm pumped MgO:$LiNbO_3$-OPA. The corresponding seed wavelength of the MIR region is also marked in the brackets.

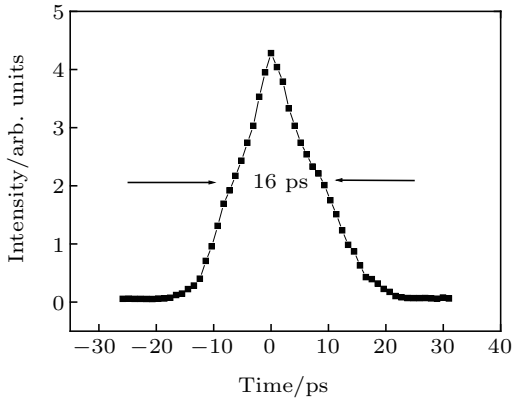


Fig. 5. Dependence of the pulse energy at a wavelength of 3.374 μm on the relative time delay between the pump of the OPA and the seeds generated from OPG.

3.2. Detection of weak MIR pulses by parametric up-conversion

Detection of MIR radiation, especially weak radiation in the MIR region, is often a problem, due to the lack of a suitable detector that can be operated at room temperature. Such a problem can be solved easily by seeding the weak MIR radiation as the idler in an MIR-OPA, such as 1064-nm or 532-nm pumped MgO:$LiNbO_3$. In the OPA, the MIR signal, on one hand, can be significantly amplified with a very large parametric gain and, in the meantime, it is also frequency up-converted to the signal in the near-IR or even visible range. The amplification and up-conversion make detection of the MIR signal very easy. More importantly, on a low seeding level, the parametric amplification is linear over a large dynamic range.

In what follows, we will test the linearity of the gain factor for the MIR pulse by adjusting the seeding energy with various optical density filters and measuring the corresponding up-conversion output energy in the near-infrared region, and then deduce the amplified signal energy in the MIR region from the Manley–Rowe equation. Figure 6 shows the relation between the amplified signal energy and the seeding energy at 3.374 μm with a fixed pump energy of 1.9 mJ for the OPA. With no attenuation of the seeder, the measured energy of the signal after amplification is 120 μJ per pulse, which is strong enough to be measured by a calibrated energy meter. Then, the intensity of seeds is attenuated step-by-step with a series of optical density filters (ODF). The amplified signal energy, which is below the detection limit of the energy meter, is detected by a fiber spectrometer (spectrum region: 0.85–2.5 μm) after calibration by an energy meter. One can see from the inset of Fig. 6 that, at a low seeding level, the intensity of the amplified signal increases almost linearly with the seeding energy changing from zero to about 1.4 pJ and starts to show a nonlinear relationship with the seeding energy more than 26 pJ. The gain eventually becomes saturated. The small signal gain factor is found to be as high as 5×10^5. While in the saturation region the amplification factor drops to an order of 10^3–10^4.

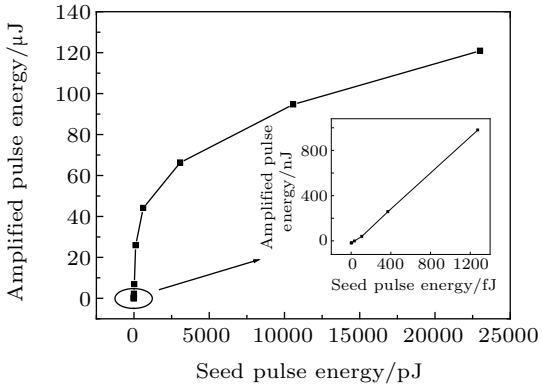


Fig. 6. Dependence of the amplified signal on the energy of the seeder in a 1064-nm pumped MgO:$LiNbO_3$-OPA with one MgO:$LiNbO_3$ crystal in the OPA stage. The insert shows the linear amplification at low seeding level.

Figure 7 shows the spectrum of the up-converted signal of the OPA at 1.554 μm under seeded and unseeded conditions with a total attenuation of about 5×10^{-8} for the seeder, corresponding to a seeding energy of 1.2 fJ per pulse at 3.374 μm. It is found that the relative amplitude of the signal is about 129 when the OPA is seeded, while the relative amplitude of the noise is about 24 when the seeder is blocked, which corresponds to a signal-to–noise (S/N) ratio of about 5:1. If the detector is cooled to reduce thermal noise, the detection limit should be even better.

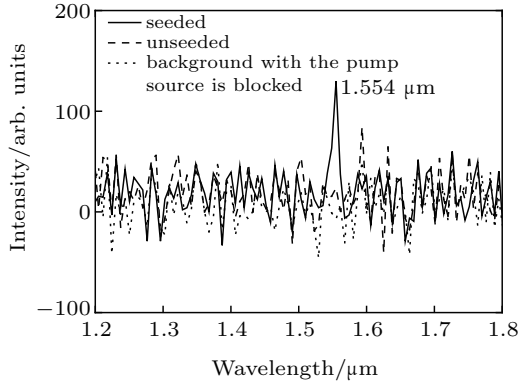


Fig. 7. Up-conversion signal spectral output of the OPA seeded at 3.374 μm and unseeded at 1.554 μm.

In order to improve the detection limit and gain factor further, another MgO:$LiNbO_3$ crystal is adopted in the OPA stage. The second MgO:$LiNbO_3$ crystal is also tilted in the opposite direction, thus the beam walk-off of the pump and signal waves in the two crystals are partially cancelled. Under the same experimental condition, the amplified pulse energy is greatly enhanced and reaches 160 μJ with no attenuation of the seeder, as shown in Fig. 8. The small gain factor increases to about 7×10^7, which is about two orders of magnitude higher than that with one MgO:$LiNbO_3$ crystal in the OPA stage. Therefore, with a two-crystal OPA, the gain factor is improved by two orders of magnitude and the signal-to-noise ratio is also expected to be improved.

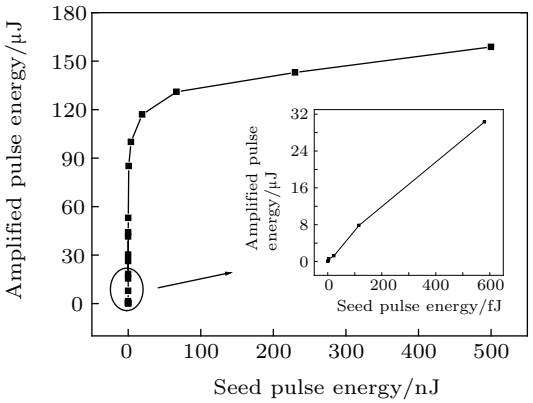


Fig. 8. Dependence of the amplified signal on the energy of the seeder in the 1064-nm pumped two MgO:$LiNbO_3$ crystals' OPA stage. The insert shows the linear amplification at a low seeding level.

Figure 9 displays the spectrum of the up-conversion signal output of the OPA at 1.554 μm under seeded and unseeded conditions with a total attenuation of about 7.7×10^{-10}, corresponding to a seeding energy of about 390 aJ per pulse at 3.374 μm. From this figure, the signal-to-noise ratio is about of 1.7:1. This corresponds to a detection limit in the MIR pulse at a wavelength of 3.374 μm less than 390 aJ per pulse before being amplified by the two-crystal OPA.

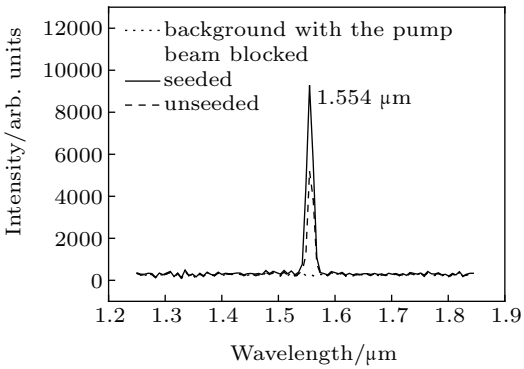


Fig. 9. Amplified and up-converted signal spectral output at 1.554 μm for seeded at 3.374 μm and unseeded in the 1064 nm pumped two MgO:$LiNbO_3$ crystals OPA.

To see the up-conversion of the MIR signal to the visible range with an OPA stage, we seeded an MIR signal at a wavelength of 3.374 μm in a 532-nm pumped MgO:$LiNbO_3$ and measured the up-converted signal at 631.5 nm. It is clear that without seeding there are some small peaks in the background from the super-fluorescence generated by the OPA. However, the peak becomes very strong when it is seeded. The amplified and up-converted beam spot can be clearly seen with a paper card and the spectrum is displayed in Fig. 10.

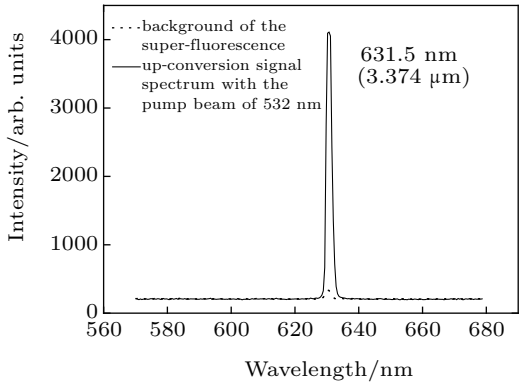


Fig. 10. The up-conversion signal spectrum at 631.5 nm with the MIR signal seeded at 3.374 μm when it is amplified in a 532 nm pumped MgO:$LiNbO_3$ OPA.

4. Conclusion

In summary, we have demonstrated the possibility of generating widely tunable, picosecond MIR coherent pulses using OPG/OPA with bulk MgO:$LiNbO_3$. Pumped by picosecond pulses at 1.064 μm, the device can be angularly tuned to yield signal and idler output in the range of 1.361–1.656 μm and 4.875–2.976 μm,

respectively. A maximum signal and idler pulse energy of 1.3 and 0.47 mJ are obtained with a MIR quantum conversion efficiency of higher than 25%. We also demonstrated the feasibility of converting ab MIR signal to the visible or near-IR range in OPA with a very high parametric gain. In a two-crystal OPA, a maximum gain factor of about 7×10^7 can be achieved at the MIR wavelength of 3.374 μm under the pumping energy of 1.9 mJ, and the corresponding energy detection limit is as low as about 390 aJ per pulse. This technique may find wide applications in the detection of weak MIR signals such as laser remote sensing and molecular spectroscopy.

References

[1] Dayan B, Pe'er A, Friesem A A and Silberberg Y 2004 *Phys. Rev. Lett.* **93** 023005

[2] Kornaszewski L W, Gayraud N, Stone J M, MacPherson W N, George A K, Knight J C, Hand D P and Reid D *Opt. Express* **15** 11219

[3] Cristian M, Roberto O, Marco M, Marcel S, Uwe M and Giulio C 2009 *Opt. Lett.* **34** 620

[4] Powers P E, Kulp T J and Kennedy R 2000 *Appl. Opt.* **39** 1440

[5] Yanagawa T, Tadanaga O, Nishida Y, Miyazawa H, Magari K, Asobe M and Suzuki H 2006 *Opt. Lett.* **31** 960

[6] Liu S D, Yang J F, He J L, Zhang B T, Yang X Q, Liu F Q, Yang H W, Xu J L and Huang H T 2011 *Laser Phys.* **21** 327

[7] Xia L Z, Su H and Ruan S C 2009 *Chin. Phys. Lett.* **7** 1038

[8] Heese C, Phillips C R, Gallmann L, Fejer M M and Keller U 2010 *Opt. Lett.* **35** 2340

[9] Yang H, Qian L J, Yuan P, Luo H and Zhu H Y 2009 *Chin. Sci. Bull.* **54** 3623

[10] Lin S and Suzuki T 1996 *Opt. Lett.* **21** 579

[11] Petrov V, Rotermund F and Noack F 1998 *Appl. Opt.* **37** 8504

[12] Lin S J, Tanaka Y, Aono M and Suzuki T 1997 *Jpn. J. Appl. Phys.* **36** 3510

[13] Carlos R B and Kevin J K 2011 *Opt. Lett.* **36** 187

[14] Zhang J Y, Shreenath A P, Kimmel M, Zeek E, Trebino R and Link S 2003 *Opt. Express* **11** 601